

Fidelity of state-of-the-art models in simulating the observed teleconnection between the Tropical South Atlantic and ISMR

Dr. Manish Kumar Joshi

(RCCS, PNU, Busan, Republic of Korea)

manishkumarjoshi@gmail.com

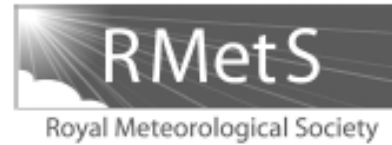
&

Dr. Fred Kucharski

(ICTP, Trieste, Italy)



The Abdus Salam
**International Centre
for Theoretical Physics**



Influence of tropical South Atlantic sea-surface temperatures on the Indian summer monsoon in CMIP5 models

Fred Kucharski^{a,b*}  and Manish K. Joshi^c

Outline

- ✧ Objectives
- ✧ Methodology
- ✧ Results
- ✧ Conclusion

Objectives

- ✧ To evaluate the fidelity of 32 CMIP5 models in simulating TSA-ISMR teleconnection.
- ✧ This study addresses the following issues:
 - Are CMIP5 models under consideration capable of simulating TSA SST variability?
 - Do CMIP5 models have capability to reproduce the TSA-ISMR teleconnection?
 - Are CMIP5 models capable of reproducing the atmospheric circulation and convergence/divergence patterns associated with TSA?
 - What are the key features that characterize the teleconnection in good compared to poor models as measured by TSA-ISMR teleconnection?

Model	Institution	Resolution (Latitude x Longitude)
BCC-CSM1-1	Beijing Climate Center, China Meteorological Administration, China	64 x 128
BCC-CSM1-1-m	Beijing Climate Center, China Meteorological Administration, China	160 x 320
BNU-ESM	College of Global Change and Earth System Science, Beijing Normal University, China	64 x 128
CCSM4	National Center for Atmospheric Research, USA	192 x 288
CMCC-CESM	Centro Euro-Mediterraneo per I Cambiamenti Climatici, Italy	48 x 96
CMCC-CMS	Centro Euro-Mediterraneo per I Cambiamenti Climatici, Italy	96 x 192
CanCM4	Canadian Centre for Climate Modelling and Analysis, Canada	64 x 128
CanESM2	Canadian Centre for Climate Modelling and Analysis, Canada	64 x 128
GFDL-CM3	Geophysical Fluid Dynamics Laboratory, USA	90 x 144
GFDL-ESM2G	Geophysical Fluid Dynamics Laboratory, USA	90 x 144
GFDL-ESM2M	Geophysical Fluid Dynamics Laboratory, USA	90 x 144
GISS-E2-H	NASA Goddard Institute for Space Studies, NY	90 x 144
GISS-E2-R	NASA Goddard Institute for Space Studies, NY	90 x 144
HadCM3	Met Office Hadley Centre, UK	73 x 96
HadGEM2-AO	National Institute of Meteorological Research/Korea Meteorological Administration, South Korea	145 x 192
HadGEM2-CC	Met Office Hadley Centre, UK	145 x 192
HadGEM2-ES	Met Office Hadley Centre, UK	145 x 192
INM-CM4	Institute for Numerical Mathematics, Russia	120 x 180
IPSL-CM5A-LR	Institut Pierre-Simon Laplace, France	96 x 96
IPSL-CM5A-MR	Institut Pierre-Simon Laplace, France	143 x 144
IPSL-CM5B-LR	Institut Pierre-Simon Laplace, France	96 x 96
MIROC4h	Atmosphere and Ocean Research Institute (The University of Tokyo), National Institute for Environmental Studies, and Japan Agency for Marine-Earth Science and Technology, Japan	320 x 640
MIROC5	Atmosphere and Ocean Research Institute (The University of Tokyo), National Institute for Environmental Studies, and Japan Agency for Marine-Earth Science and Technology, Japan	128 x 256
MIROC-ESM	Japan Agency for Marine-Earth Science and Technology, Atmosphere and Ocean Research Institute (The University of Tokyo), and National Institute for Environmental Studies, Japan	64 x 128
MIROC-ESM-CHEM	Japan Agency for Marine-Earth Science and Technology, Atmosphere and Ocean Research Institute (The University of Tokyo), and National Institute for Environmental Studies, Japan	64 x 128
MPI-ESM-LR	Max Planck Institute for Meteorology (MPI-M), Germany	96 x 192
MPI-ESM-MR	Max Planck Institute for Meteorology (MPI-M), Germany	96 x 192
MPI-ESM-P	Max Planck Institute for Meteorology (MPI-M), Germany	96 x 192
MRI-CGCM3	Meteorological Research Institute, Japan	160 x 320
MRI-ESM1	Meteorological Research Institute, Japan	160 x 320
NorESM1-M	Norwegian Climate Centre, Norway	96 x 144
NorESM1-ME	Norwegian Climate Centre, Norway	96 x 144

Table List of CMIP5 models along with their modeling groups and resolution

Methodology

- ✧ To examine TSA-ISMR teleconnections, the TSA index (area-averaged SSTAs over 30°W – 10°E , 20°S – 0°) is used.
- ✧ Because of possible co-variability with ENSO:
 - Linear relation between the two, obtained by regressing the TSA index onto Niño 3.4 index (area-averaged SSTAs over 170°W – 120°E , 5°S – 5°N), has been removed from TSA (*Kucharski et al. 2008*).
- ✧ Resulting TSAR is linearly independent from Niño 3.4 index and therefore be used as an ENSO-independent index that could influence the Indian monsoon.

Precipitation Simulation

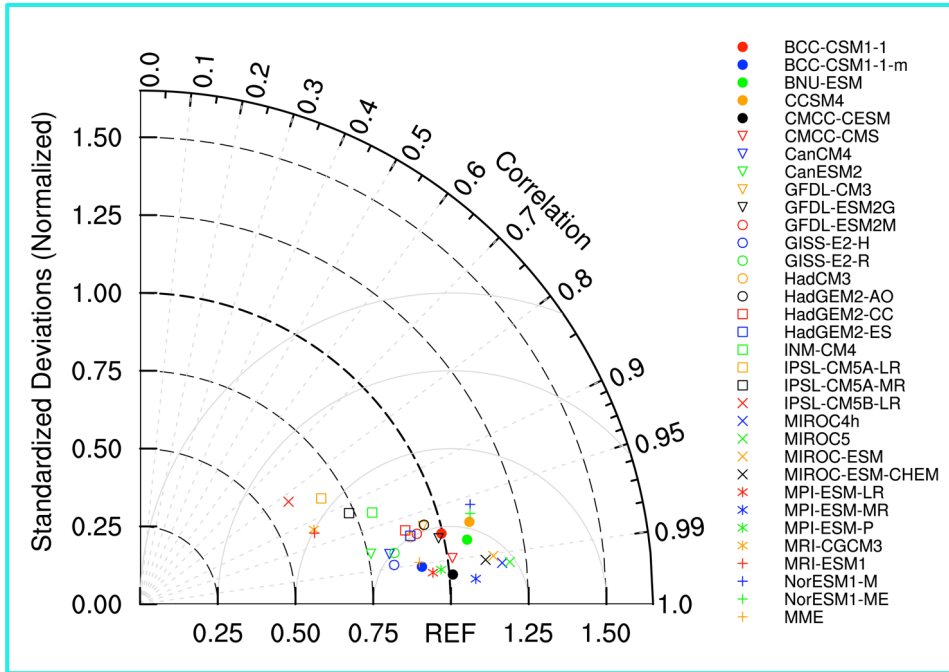


Fig. Annual cycle, representing the climatological monthly mean of precipitation area-averaged over the monsoon core region (10°N to 30°N, 70°E to 100°E).

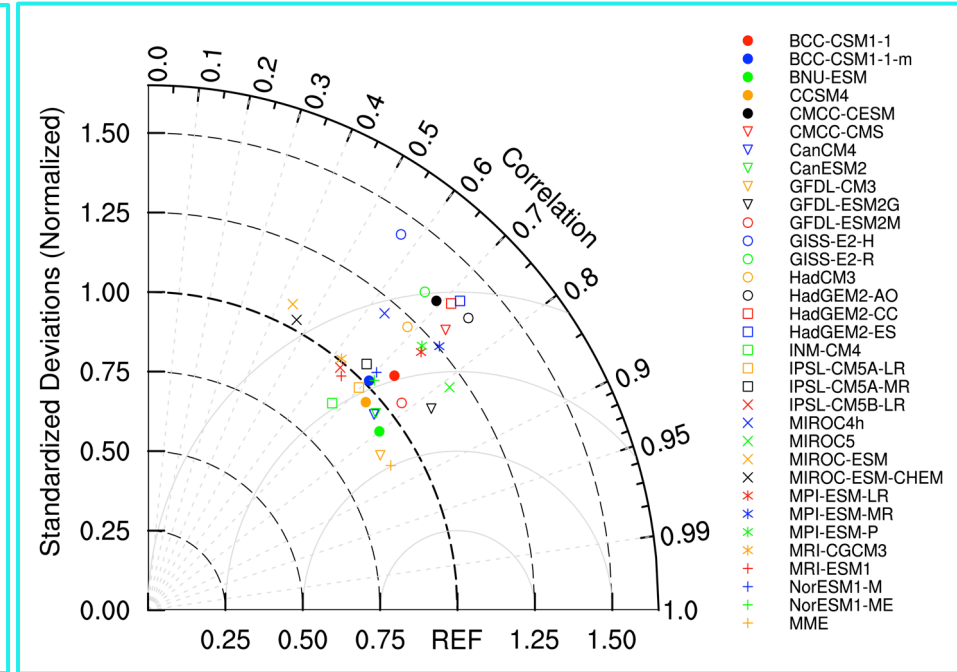


Fig. Spatial pattern of climatological seasonal (JJAS) mean precipitation over the Indian monsoon region (15°S to 30°N, 50°E to 120°E).

- ✧ Except IPSL-CM5B-LR and IPSL-CM5A-LR, all other models show a CC > 0.9.
- ✧ But, some either underestimate or overestimate the variance.
- ✧ In terms of both magnitude and phase, the models BCC-CSM1-1, CMCC-CESM, CMCC-CMS, GFDL-ESM2G, MPI-ESM-LR, MPI-ESM-MR, and MPI-ESM-P are very close to the observation and hence, simulate the best annual cycle as compared to other models.

- ✧ Most of the models show good CCs.
- ✧ Criteria to identify models: CC > 0.6 and normalized SD lying between 0.75 and 1.25.
- ✧ Based on this criterion, the models MIROC-ESM and MIROC-ESM-CHEM have lowest CC, while the models GISS-E2-H, GISS-E2-R, CMCC-CESM, CMCC-CMS, HadGEM2-AO, HadGEM2-CC, HadGEM2-ES, and MPI-ESM-MR are highly overestimating the climatological seasonal mean precipitation.

- ✧ Models are not selected based on the above criterion for the analysis of TSA-ISMR teleconnection, because all models are to some extent able to reproduce the:
 - ISMR seasonal cycle and
 - Climatology
- ✧ Also, a selection would involve the risk of excluding models from further analysis because of ad-hoc and subjectively chosen thresholds.

TSA Pattern Simulation

- Most of the models show well-defined spatial pattern of TSA, localized over the south tropical Atlantic and having magnitudes quite comparable to the observed one.
- More than 65% of models (21) also show -ve anomalies over the South Atlantic region (centered around 30°S).
- Referred as SAOD (Nnamchi *et al.* 2011, 2016).

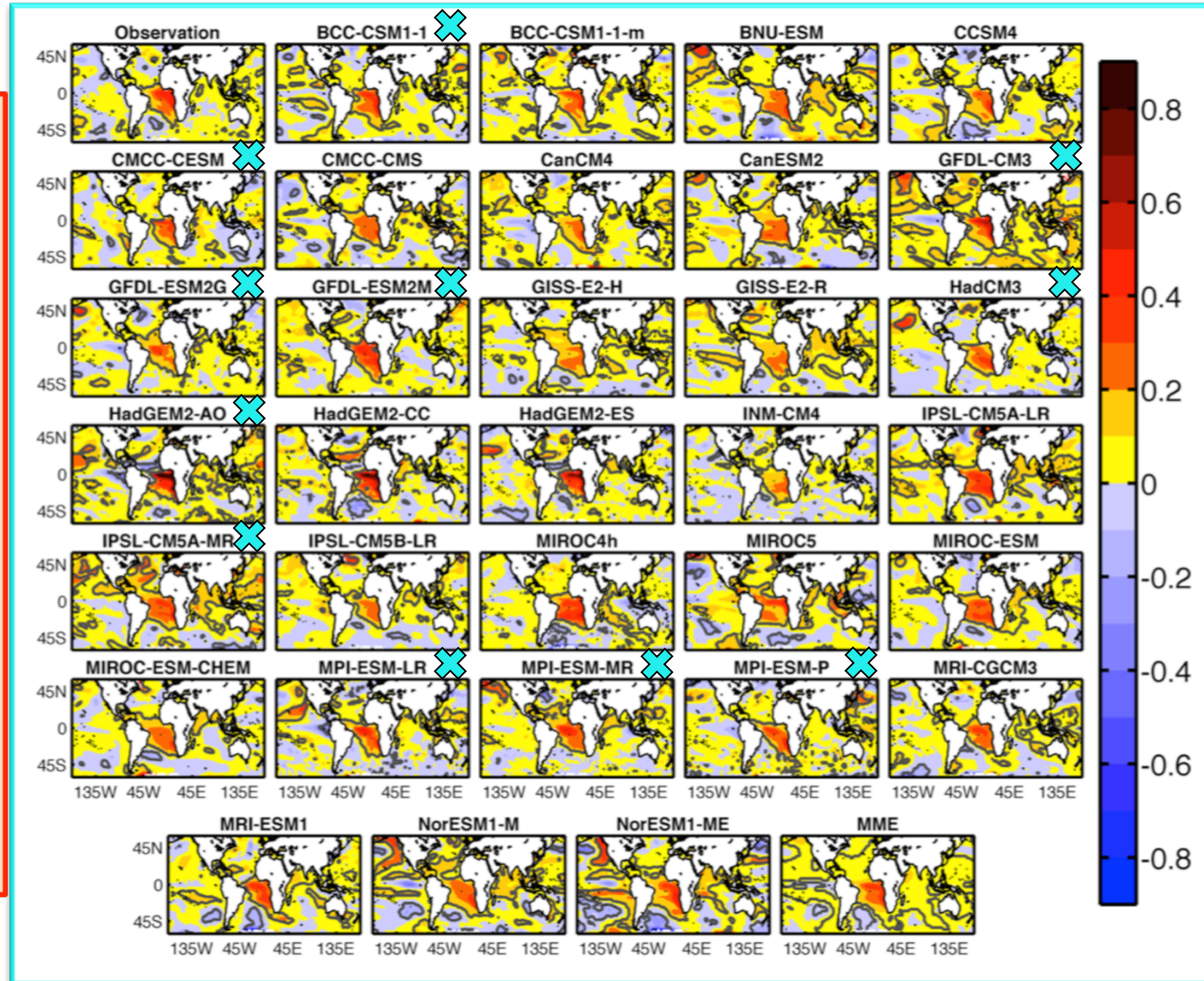


Fig. Regression maps of JJAS SSTAs onto the standardized TSAR (units are °C per standard deviation) for observation and 32 CMIP5 models. The grey contours in observation and CMIP5 models indicate the regions where the regression coefficient is statistically significant at 95% CL.

Taylor Diagram of TSA-R-SST Regressions

- ◇ All models show $CC > 0.7$.
- ◇ HadGEM2-AO, HadGEM2-CC, & HadGEM2-ES highly overestimate the variance, while CanCM4, INMCM4, GISS-E2-H, GISS-E2-R, & IPSL-CM5B-LR highly underestimates.

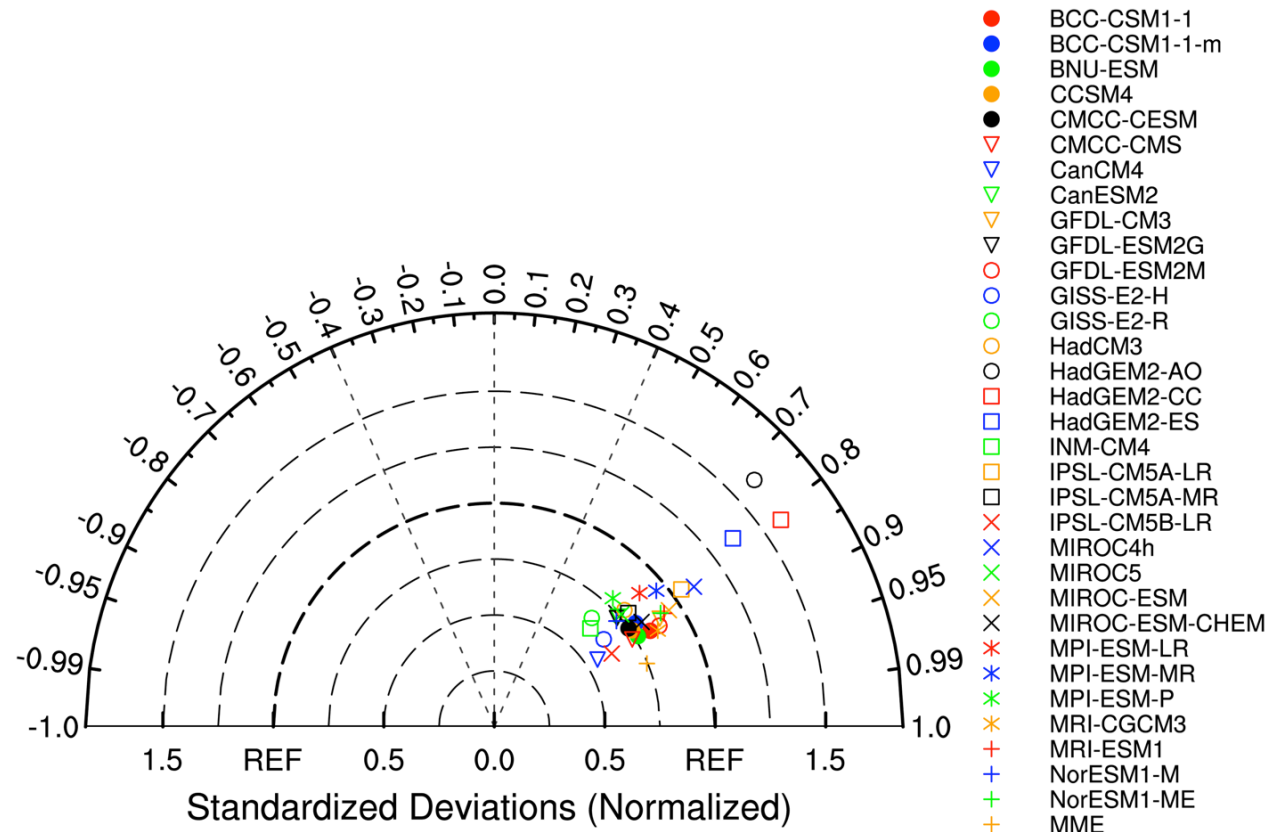


Fig. Taylor diagram of spatial TSA-SST regression pattern, obtained by regressing SSTAs onto the standardized TSA, over the Atlantic domain (40°S–40°N, 60°W–10°E).

Overall, SST regression patterns & its Taylor Diagram reveals that CMIP5 models are capable of simulating the TSA pattern.

TSA-ISM_R Teleconnection

✧ Warm SSTAs over TSA:

- Reduction of rainfall: - CI
- Enhancement of rainfall: - Eastern India.

✧ The observed precipitation regression shows a dipolar pattern, i.e.,

- -ve anomalies over CI &
- +ve over EI (especially near Bangladesh).

✧ Models show diverse behavior.

✧ Some models show similar regression patterns as seen in the observations (e.g., CMCC-CMS, GFDL-ESM2G, MIROC5), while others show opposite pattern (e.g., GFDL-ESM2M, MPI-ESM-MR) or weak responses.

✧ Consistent with observations, MME (averaged across all models) also shows a dipolar pattern, but the signal is weak.

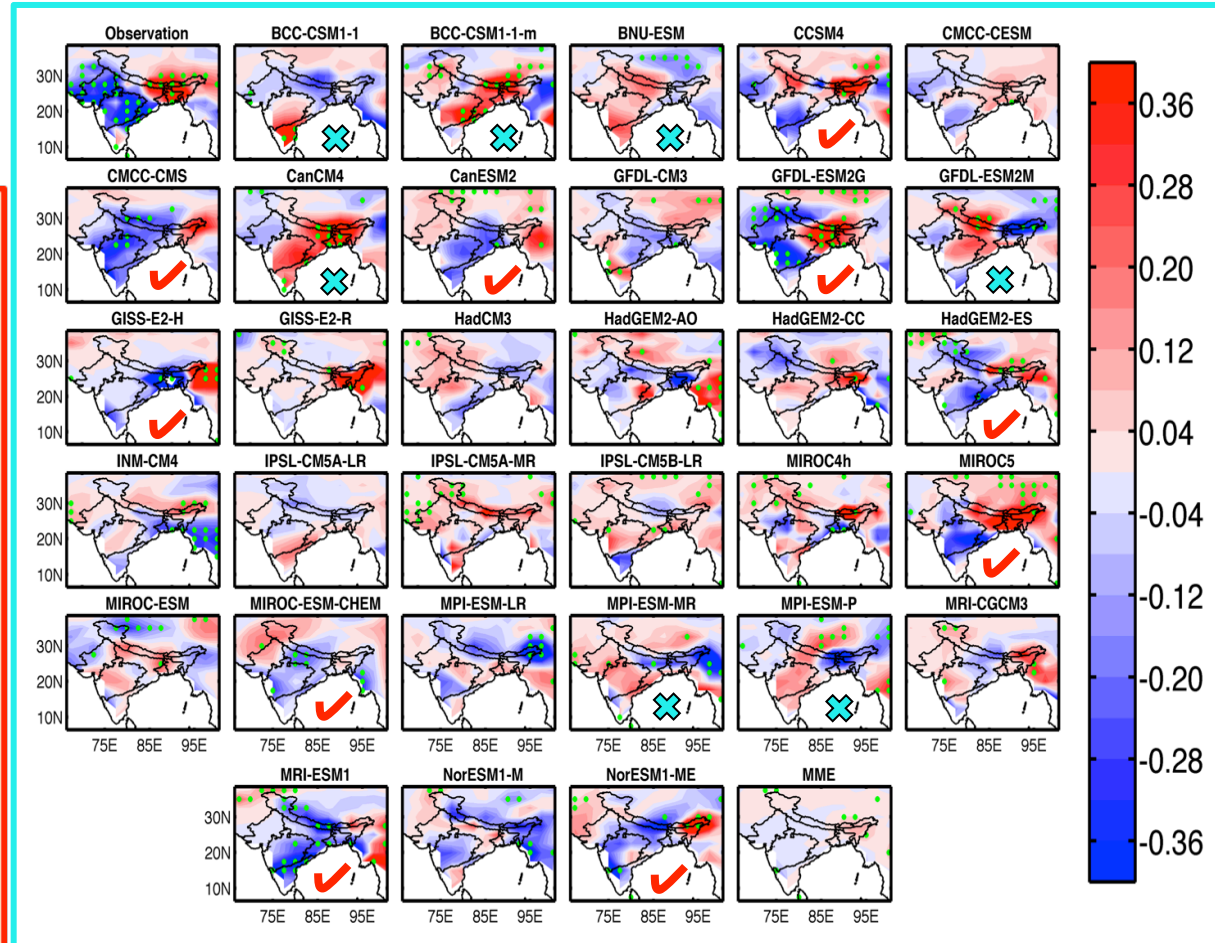


Fig. Regression maps of JJAS precipitation anomalies onto the standardized TSA_R (units are mm/d per standard deviation) for observation and 32 CMIP5 models. The green stippling in observation and CMIP5 models indicates the grid point where the regression coefficient is statistically significant at 90% CL, which is assessed via a two-tailed t test.

Categorization of Models

✧ Based on the sign of average regression coefficients, models are categorized into two groups:

- Good (-ve) &
- Poor (+ve).

✧ The ensemble mean of good models closely resembles to the observation.

NOTE

✧ Classification of models into good & poor categories is solely based on the matrix of TSA-ISMIR regressions, and is not related to the overall model performance.

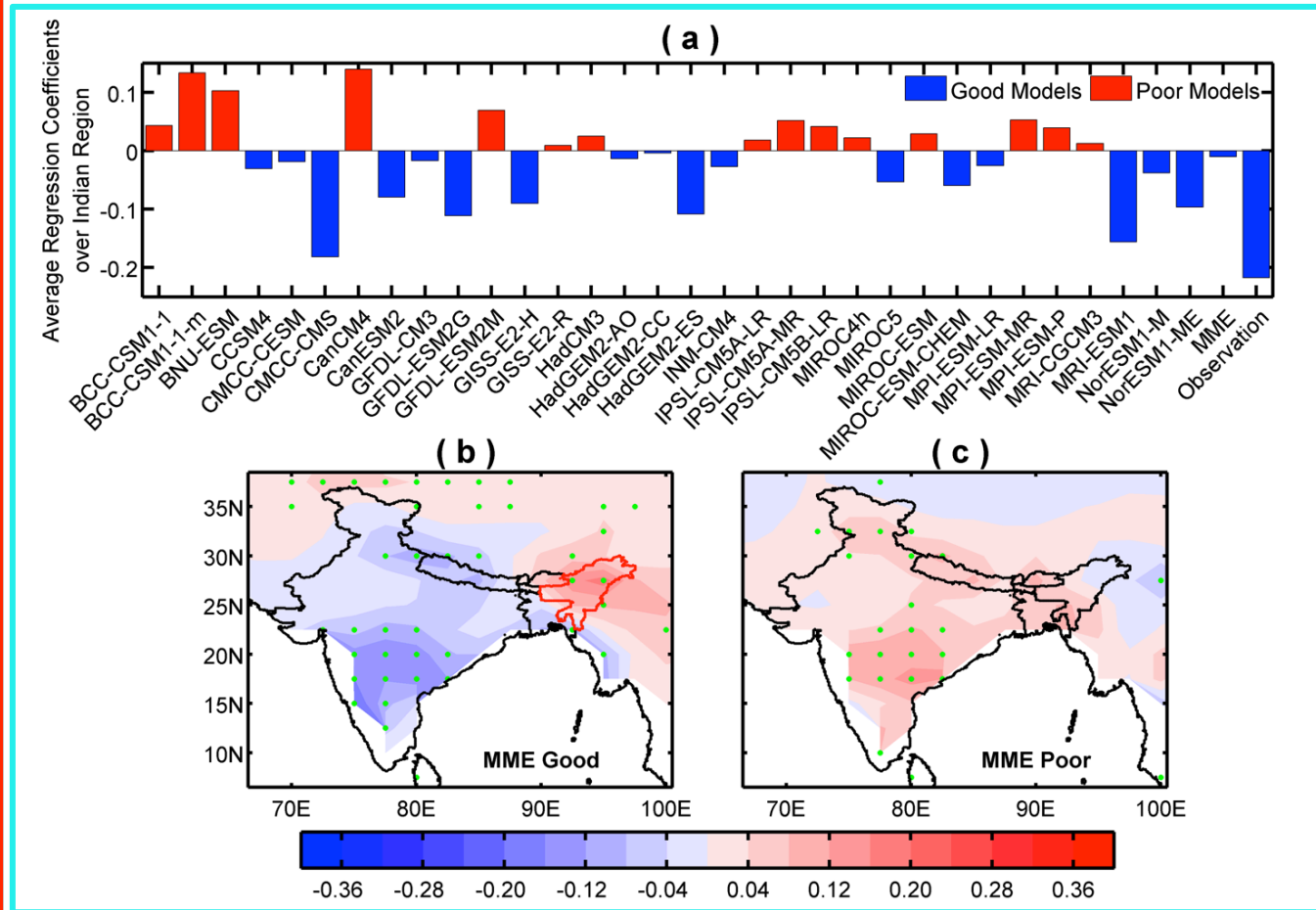


Fig. a Area average of the TSAR precipitation regression maps over Indian land points, excluding northeast region. **b** and **c** Ensemble means of the TSAR precipitation regression patterns of 17 good (MME good) and 15 poor (MME poor) CMIP5 models, respectively. The green stippling in MME good and MME poor indicates the grid points where the regressions are statistically significant at the 90% CL.

✧ To get further insight of crucial elements in model TSA pattern, ensemble means of good & poor models constructed.

✧ Consistent with Observations, both models show a dipole structure, i.e.,

- Warming over TSA & equator.
- Cooling in southern subtropical Atlantic (around 30°S).
- Referred as SAOD (Nnamchi et al. 2011, 2016).

✧ Negative pole of this dipole is slightly more pronounced & closer to observations in good models.

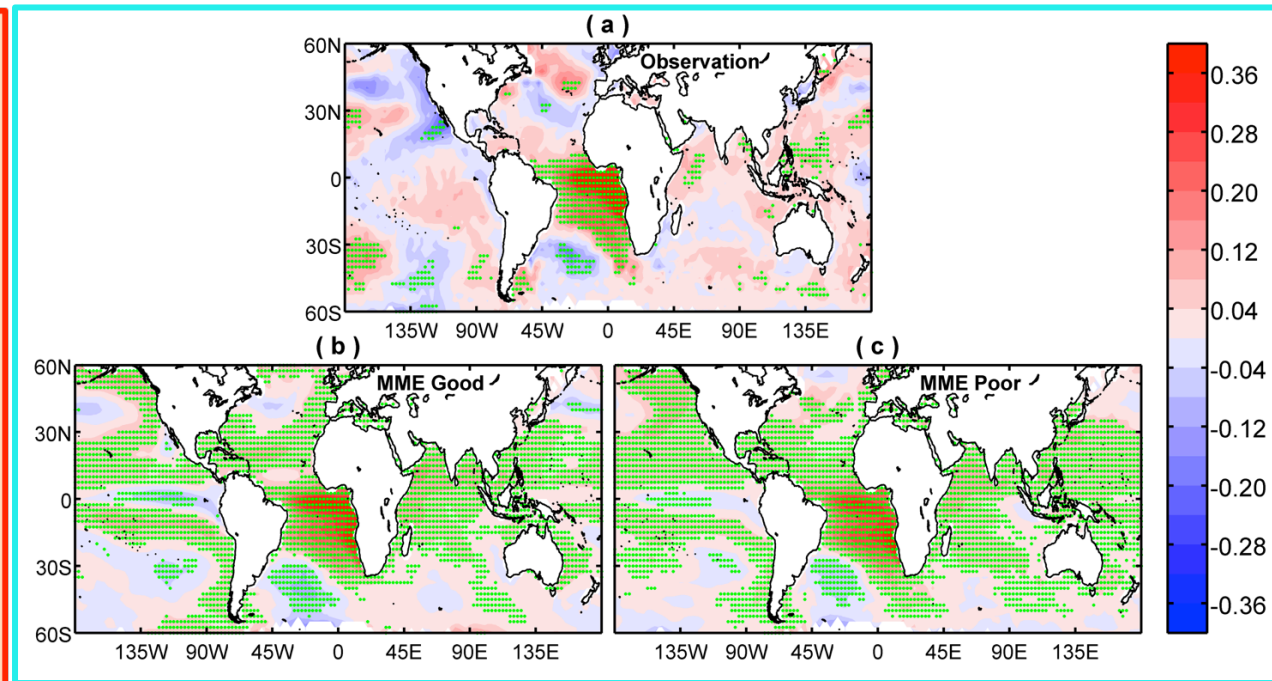


Fig. a Observed TSAR SST regression pattern. **b** and **c** Ensemble means of the TSAR SST regressions of good (MME good) and poor (MME poor) CMIP5 models, which are computed by averaging the regression maps of SSTAs onto the standardized TSAR across all 17 good and 15 poor models. The green stippling in MME good and MME poor indicates the grid point where the sign of regression coefficient is statistically significant at 95% CL.

✧ Looking at TSA-SST pattern it is difficult to guess

- What distinguishes good from poor models?
- Therefore, the atmospheric features are examined further to get some clue.

*Capability of CMIP5 models in
reproducing the Atmospheric
Circulation and the
Convergence/Divergence patterns
associated with TSA*

TSA-Winds Regression Pattern (850 hPa)

- ✧ Warm SSTAs over TSA is associated with westerly anomalies along the equator, located slightly northward.
 - This response is stronger and closer to the observations in good models.
- ✧ Easterly wind anomalies over Africa & in the Somali Jet region; consistent with a Gill-type response (heating induced by TSA warming).
 - Poor models fail to reproduce this feature & show stronger response in EIO.
 - Consistent with increased convergence over India.
- ✧ This weakened Somali jet reduces rainfall over India
 - Through divergence &
 - Due to reduced lifting at Western Ghats.
- ✧ A cyclonic feature in the extratropical South Atlantic region, which is a part of the SAOD (Nnamchi et al. 2011, 2016).
 - Captured by both good & poor models.

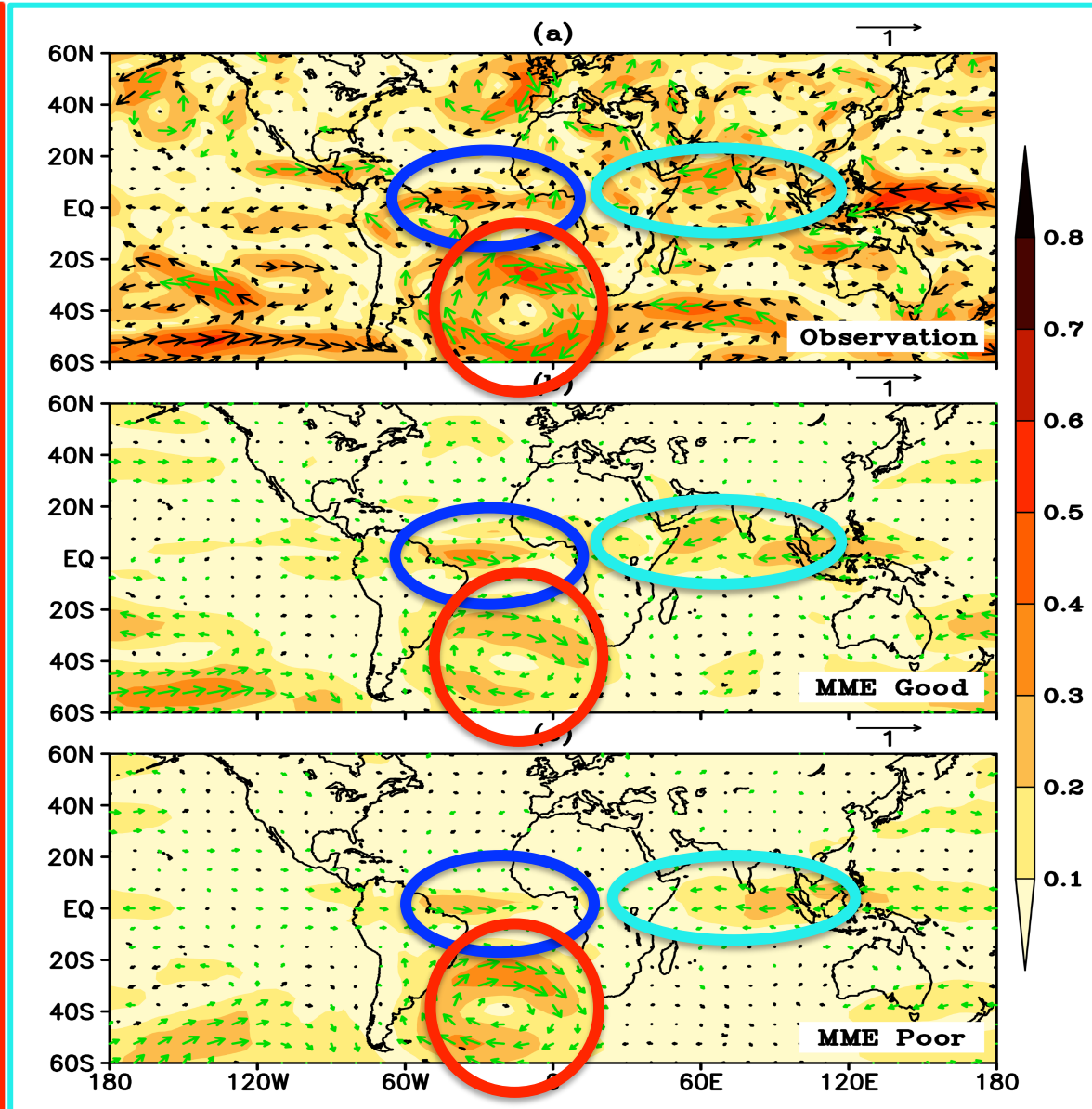


Fig. (a) Regression of JJAS seasonal anomalies of zonal and meridional winds at 850 hPa onto the standardized TSAR. (b) and (c) Same as in (a), but for the averaged regressions of 17 good and 15 poor CMIP5 models, respectively.

TSA-Winds Regression Pattern (200 hPa)

✧ At upper levels, equatorial response is reversed, consistent with a baroclinic response.

- Reproduced by both (Good & Poor).
- Ensemble mean of good models show strong signal over western IO, as seen in observation.

✧ An extratropical wave-train-type feature in the Northern Hemisphere.

- Absent in both good & poor models.
- This extratropical pathway may be the cause for the reduction of rainfall over NW India, allied with TSA anomaly, as seen in observed precipitation regression, but absent in good models (Yadav 2017).

✧ At lower & upper levels: outstanding feature in IO (particularly in the Somali Jet region) is the baroclinic response, which is well captured by good models.

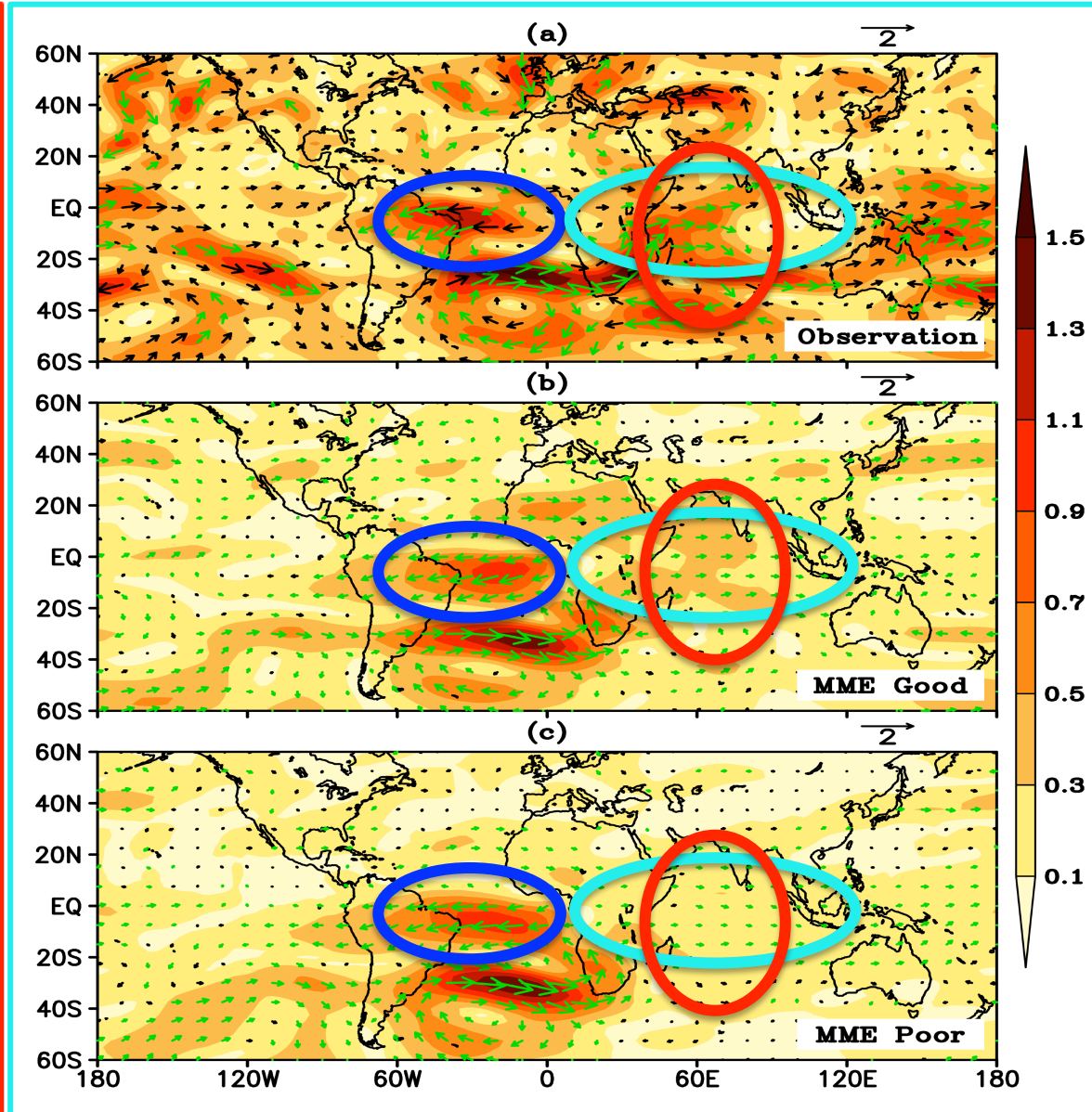


Fig. (a) Regression of JJAS seasonal anomalies of zonal and meridional winds at 200 hPa onto the standardized TSAR. (b) and (c) Same as in (a), but for the averaged regressions of 17 good and 15 poor CMIP5 models, respectively.

TSA-Eddy Stream Function Regression Pattern (200 hPa)

- ✧ A good indicator of Gill response to TSA SST anomaly is Eddy-SF regression at 200hPa.
- ✧ Observed regression pattern shows Gill-type quadrupole response, which is up to some extent captured by both (Good & Poor).
 - Compared with Poor models, good models show more pronounced and localized (i.e., stronger amplitudes in the Saudi Arabian peninsular region) quadrupole eddy SF response.

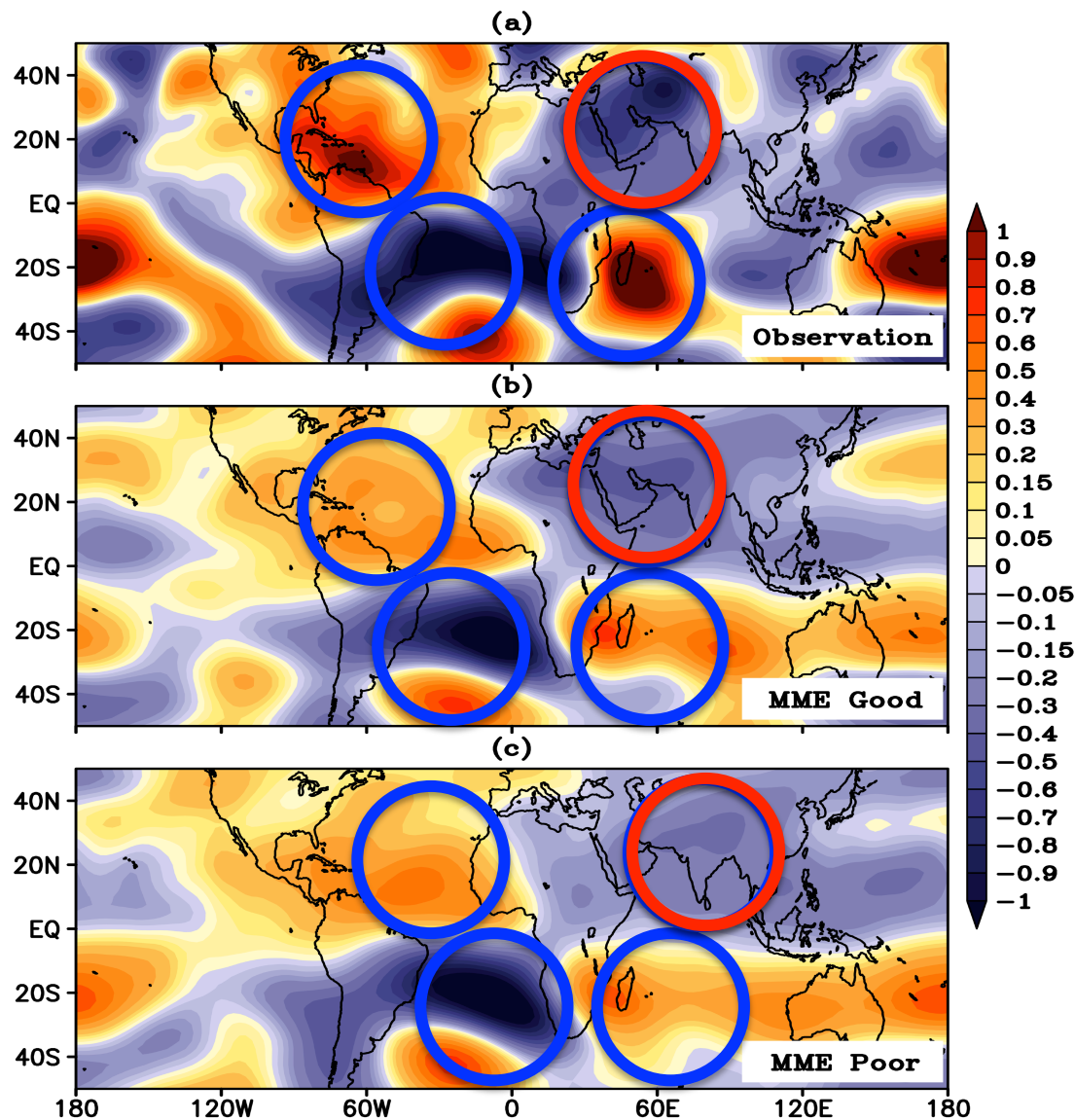


Fig. (a) Regression of JJAS anomaly of eddy stream function at 200 hPa from NCEP/NCAR reanalysis (1951–2004) onto the standardized TSAR. (b) and (c) Same as in (a), but for the averaged regressions of 17 good and 15 poor CMIP5 models, respectively. The unit of eddy stream function is $10^6 \text{ m}^2 \text{ s}^{-1}$ per standard deviation.

TSA-Eddy Stream Function Regression Pattern (850 hPa)

- ✧ At lower levels, TSA Eddy SF regressions also show a quadrupole, but with opposite sign (consistent with a baroclinic Gill-type response).
- ✧ Both observations & good models show low-level anticyclonic SF over Arabian Sea, extending to India.
 - Induce sinking motion & low-level divergence that causes reduction of rainfall.
- ✧ Poor models also show a quadrupole response, but the center over Arabian Sea, extending towards India is missing.
 - Located in EIO & WP.
 - Consistent with low-level wind responses.

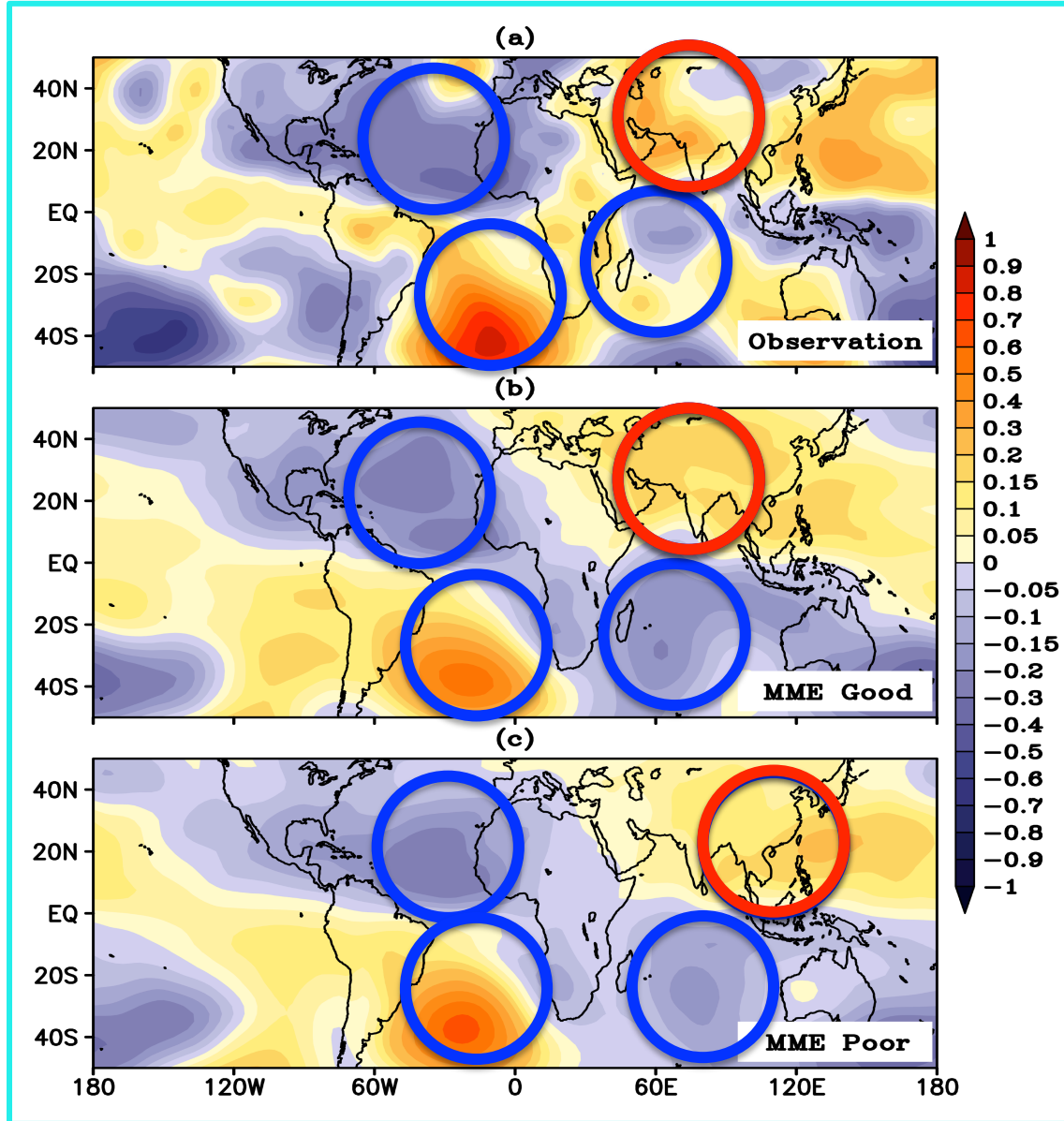


Fig. (a) Regression of JJAS anomaly of eddy stream function at 850 hPa from NCEP/NCAR reanalysis (1951–2004) onto the standardized TSAR. (b) and (c) Same as in (a), but for the averaged regressions of 17 good and 15 poor CMIP5 models, respectively. The unit of eddy stream function is $10^6 \text{ m}^2 \text{ s}^{-1}$ per standard deviation.

TSA-Velocity Potential Regression Pattern (200 hPa)

- ❖ Warm SSTAs over TSA is associated
 - Anomalous convergence: Indian sub-continent, WP & far EP.
 - Divergence: tropical Atlantic & C-E Pacific at upper levels.
 - With anomalous divergence and convergence over respective regions at lower levels.
- ❖ Ensemble mean of poor models fail to show the convergence over Indian sub-continent & divergence over C-E Pacific at upper levels.
 - In fact it shows stronger convergence over C-E Pacific and weaker convergence in WP at upper levels.
- ❖ Such differences in large-scale features may be responsible for difference in TSA-ISM R teleconnection in both (Good & Poor).

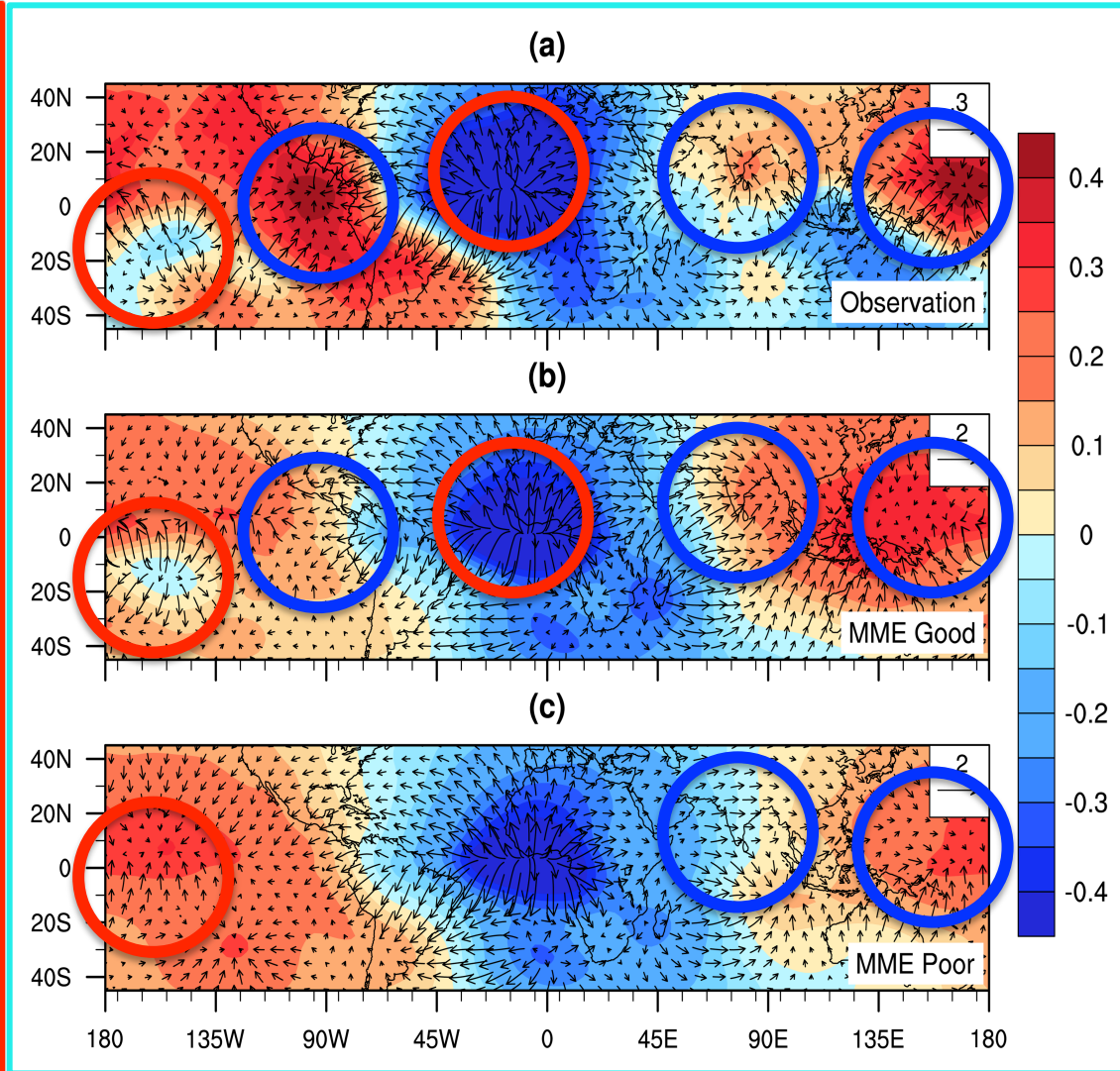


Fig. (a) Regression of JJAS anomaly of velocity potential at 200 hPa from NCEP/NCAR reanalysis (1951–2004) onto the standardized TSAR. (b) and (c) Same as in (a), but for the averaged regressions of 17 good and 15 poor CMIP5 models, respectively. The unit of velocity potential is $10^6 \text{ m}^2 \text{ s}^{-1}$ per standard deviation. The vectors represent the divergent wind (m s^{-1}).

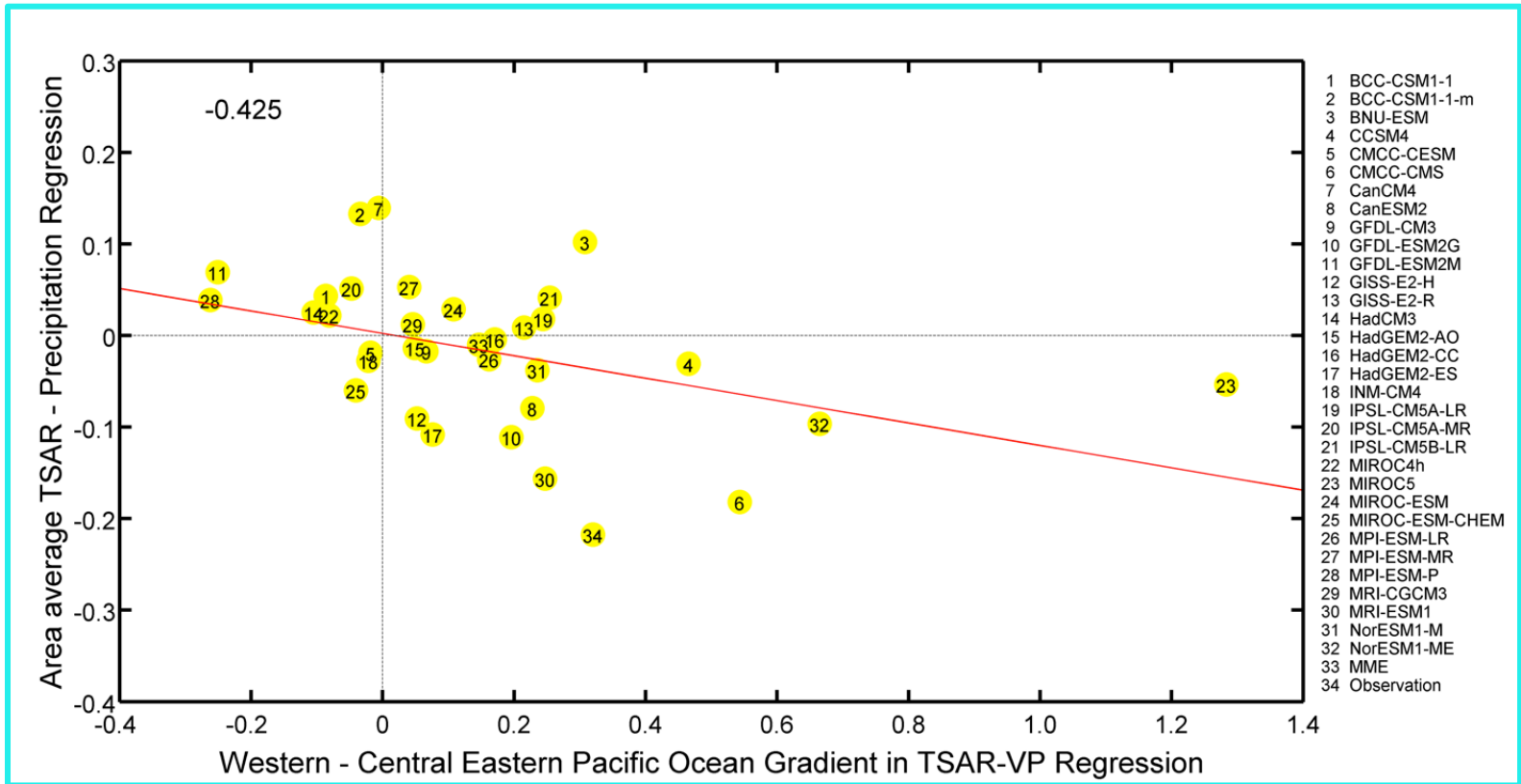


Fig. Scatter plot of TSAR precipitation regressions (units are mmday^{-1} per standard deviation) averaged over Indian land points, excluding the northeast region, versus western ($140^{\circ}\text{--}180^{\circ}\text{E}$, $0\text{--}20^{\circ}\text{N}$) – central eastern ($170^{\circ}\text{W}\text{--}130^{\circ}\text{W}$, $20^{\circ}\text{S}\text{--}0^{\circ}$) Pacific Ocean Gradient in TSAR velocity potential (200 hPa) regressions.

✧ Strong relationship between the quality of reproducing the VP regression pattern and the TSAR-ISMIR teleconnection in models.

Conclusion

- ✧ Generally, all models show well-defined spatial pattern of TSA:
 - But, only 50% are able to capture the TSA-ISMR teleconnection.
- ✧ Both good & poor models show large-scale responses, which is quite consistent with observations.
- ✧ Large-scale Walker circulation adjustment to the TSA SSTAs:
 - Is identified as one of the factors that account for the differences in the low-level SF response.
- ✧ Results reveal strong relationship between the quality of reproducing the VP regression pattern and the TSA-ISMR teleconnections in models:
 - In particular w. r. t. the western & central-eastern Pacific Ocean velocity potential gradients at 200 hPa.
- ✧ Such relatively subtle changes in the response lead to a reversal of the rainfall signal over India:
 - Raises the question about the robustness of the TSA–ISMR teleconnections.

Thank You